Design and operation of membrane distillation with feed recirculation for high recovery brine concentration

Citation: Swaminathan, Jaichander, and John H. Lienhard. "Design and Operation of Membrane Distillation with Feed Recirculation for High Recovery Brine Concentration." Desalination 445 (November 2018): 51–62.

As Published: https://doi.org/10.1016/j.desal.2018.07.018

Publisher: Elsevier

Persistent URL: http://hdl.handle.net/1721.1/118409

Version: Author's final manuscript: final author's manuscript post peer review, without publisher's formatting or copy editing

Design and operation of membrane distillation with feed recirculation for high recovery brine concentration*

Jaichander Swaminathan and John H. Lienhard V*

Rohsenow Kendall Heat and Mass Transfer Laboratory, Department of Mechanical Engineering, Massachusetts Institute of Technology, Cambridge MA 02139-4307 USA

Abstract

Thermal-energy-driven desalination processes such as membrane distillation (MD), humidification dehumidification (HDH), and multi-stage flash (MSF) can be used to concentrate water up to saturation, but are restricted to low per-pass recovery values. High recovery can be achieved in MD through feed recirculation. In this study, several recirculation strategies, namely batch, semibatch, continuous, and multistage, are compared and ranked based on flux and energy efficiency, which together influence overall cost. Batch has higher energy efficiency at a given flux than semibatch and continuous recirculation because it spends more operating time treating lower salinity water for the same value of overall recovery ratio. Multi-stage recirculation is a steady-state process that can approach batch-like performance, but only with a large number of stages. Feed salinity rises during the batch operating cycle, and as a result feed velocity may have to be increased to avoid operating above the critical specific area wherein both GOR and flux are low due to significant heat conduction loss through the membrane. Finally, the choice of optimal membrane thickness for batch operation is compared to that of continuous recirculation MD.

Keywords: membrane distillation, high recovery, batch operation, energy efficiency and flux

*Corresponding author: lienhard@mit.edu

*Citation: J. Swaminathan and J.H. Lienhard V, Design and operation of membrane distillation with feed recirculation for high recovery brine concentration, *Desalination*, 445:51-62, 1 November 2018. https://doi.org/10.1016/j.desal.2018.07.018

Nomenclature

Roman Symbols

A	Area, m^2
AGMD	Air gap membrane distillation
B	Membrane permeability, kg/m^2·s·Pa
B_0	Membrane permeability coefficient, kg/m·s·Pa
c_w	Specific cost of pure water, \$/m^3
c_f	Specific cost per unit of feed treated, \$/m^3
C	Cost factor, \$/m^3 (heating, cooling) or \$·kg/m^5·s (flux)
c_p	Specific heat capacity, J/kg-K
d	Depth or thickness, m
CGMD	Conductive gap membrane distillation
DCMD	Direct contact membrane distillation
GOR	Gained Output Ratio = $\dot{m}_p h_{fg}/\dot{Q}_h$
h	Heat transfer coefficient, W/m^2·K
h_{fg}	Enthalpy of vaporization, J/kg
HDH	Humidification dehumidification
HX	Heat Exchanger
J	Permeate flux, kg/m^2 s
k	Thermal conductivity, W/m·K
L	Length of module, m
M	Mass, kg
MD	Membrane distillation
MVC	Mechanical vapor compression
$\dot{m}$	Mass flow rate, kg/s
N_{stages}	Number of stages
NTU	Number of transfer units
Nu	Nusselt number
Pr	Prandtl number
$\dot{Q}$	Heat transfer, W
Re	Reynolds number
RR	Recovery ratio of cycle
$RR_{per\text{-}pass}$	Recovery ratio per-pass through system
s	Salt concentration, g/kg
t	Time, s
t^*	Non-dimensional time

T	Temperature, °C
TTD	Terminal temperature difference, °C
U	Overall heat transfer coefficient, W/m^2·K
v	Velocity, m/s
V_0	Volume of recirculation loop, m^3
$\dot{V}$	Volume rate, m^3/s
w	Width, m

Greek Symbols

α	$d\rho/ds$, kg^2/g·m^3
δ_{m}	Membrane thickness, μm
Δ	Difference
μ	Viscosity, Pa·s
ρ	Density, kg/m^3
τ	Cycle time, s

Subscripts, Superscripts

b	Brine
c	Cold
ch	Feed/cold channel
cond	Conduction
crit	Critical value
eff,m	Effective membrane property
f	Feed channel
h	Hot/heater
i	Initial
HX	Heat exchanger
in	Inlet
m	Membrane
max	Maximum
MD	Membrane distillation module
min	Minimum
mu	Make up
out	Outlet
p	Permeate
pw	Pure water
$(\overline{\quad})$	Average over a cycle, see Eqs. (4)-(5)

1. Introduction

Conventional brackish and seawater reverse osmosis systems are not readily applied for further concentration, towards zero-liquid-discharge, of desalination brines, produced water from hydraulic fracturing, and industrial effluents. Thermal-energy-driven technologies such as membrane distillation (MD) and humidification dehumidification (HDH) are considered to be promising for such brine concentration applications as they can operate at ambient pressure and relatively low temperatures. These brine concentration applications are characterized by a high recovery ratio requirement. However, MD (except multi-effect designs) is restricted to a low value of per-pass recovery ratio, necessitating some form of brine recirculation.

In this study, we will

1. compare energy efficiency and pure water flux of various recirculation designs (batch, semibatch, continuous and multi-stage) for brine concentration.
2. elucidate the value of a control scheme that avoids counter-productive conditions characterized by high heat conduction losses across the membrane towards the end of the batch cycle as feed salinity increases.
3. comment on the choice of optimal membrane thickness for a batch recirculation system, and compare its performance against a similarly optimized continuous recirculation process.

1.1. Motivation for high product recovery

MD systems without recirculation have a low recovery ratio (RR). RR is the fraction of incoming feed water separated as pure water:

$$\mathrm{RR} = \frac{M_{\mathrm{permeate}}}{M_{\mathrm{feed}}} \tag{1}$$

where M_{permeate} is the mass of permeate produced and M_{feed} is the mass of feed to treated. Instantaneous or per-pass recovery ratio through the MD module (which is achieved without recirculation) can be defined in terms of the pure water production rate ($\dot{m}_{\mathrm{p}}$) and feed inflow rate ($\dot{m}_{\mathrm{f}}$) as $\mathrm{RR}_{\text{per-pass}} = \dot{m}_{\mathrm{p}}/\dot{m}_{\mathrm{f}}$. If ΔT_{c} denotes the change in temperature along the length of the cold (preheat) stream, applying energy conservation for the preheated feed stream gives $\dot{m}_{\mathrm{f}} c_{\mathrm{p}} \Delta T_{\mathrm{c}} = \dot{m}_{\mathrm{p}} h_{\mathrm{fg}} + \dot{Q}_{\mathrm{m,cond}}$, where $\dot{Q}_{\mathrm{m,cond}}$ is the heat transferred by conduction across the membrane. Since $\dot{Q}_{\mathrm{m,cond}} > 0$ and $\Delta T_{\mathrm{c}} < T_{\mathrm{h,in}} - T_{\mathrm{c,in}}$,

$$\mathrm{RR}_{\text{per-pass}} < \frac{c_{\mathrm{p}} \left(T_{\mathrm{h,in}} - T_{\mathrm{c,in}}\right)}{h_{\mathrm{fg}}} \tag{2}$$

MD is operated at a top temperature below 100°C, often in combination with low-temperature heat sources. If the ambient temperature is 25°C, $\mathrm{RR}_{\mathrm{per-pass}} < 13\%$. In practice (e.g., [1]) the recovery with single-pass MD without recirculation is much lower, around 8% due to a lower $T_{\mathrm{f,in}}$ and boiling point elevation of the salty feed stream leading to higher $\dot{Q}_{\mathrm{m,cond}}$.

In contrast, in order to achieve zero-liquid-discharge, the desalination process would have to concentrate the salt solution up to saturation concentration (260 g/kg for NaCl), at which point the solution could be

passed to a crystallizer. In this study, we will focus on desalinating a NaCl feed solution at 70 g/kg up to 260 g/kg. The corresponding required recovery ratio is $1 - 70/260 = 72.1\%$, much higher than the limiting value for a single-pass system. In order to implement such a high RR in a hypothetical single-pass MD process, the feed stream would have to be heated up to 500°C, after being pressurized to prevent boiling. Our focus is on more practical, alternatives configurations with feed recirculation.

1.2. Options for high recovery with MD

The following operation strategies enable high overall pure water recovery employing a low-recovery single stage process:

(a) batch recirculation

(b) semibatch recirculation

(c) continuous recirculation

(d) continuous multi-stage recirculation

Figure 1 shows a schematic representation of these alternatives.

Continuous recirculation [Fig. 1(c)] is operated such that the brine leaving the MD module is at the required final brine salinity, and is continuously bled out of the system. In order to produce this output brine salinity, the inlet salinity to the desalination process has to be: $s_{\mathrm{h,in}} = s_{\mathrm{b,out}} \times (1 - \mathrm{RR}_{\text{per-pass}}) = s_{\mathrm{f,in}} \times \frac{1-\mathrm{RR}_{\text{per-pass}}}{1-\mathrm{RR}}$. For the brine concentration application considered in this study, since $\mathrm{RR} > \mathrm{RR}_{\mathrm{per-pass}}$, the recirculated feed entering the MD module is at a higher salinity than the original feed stream. The remaining brine flow after bleed out is mixed with an appropriate quantity of incoming make-up feed to reach this inlet salinity at the module inlet.

In the MD literature, continuous recirculation has been a popular method for achieving high product recovery ratio because it is a steady-state process that is easy to implement and evaluate [2, 3, 4, 5]. Recently, Lokare et al. [6] identified and evaluated the negative impact of continuous recirculation on both energy consumption and flux.

The multi-stage recirculation process illustrated in Fig. 1(d) combines several single stage recirculation systems in series. Multi-stage recirculation also operates at steady-state and achieves a high overall RR. The first stage (on the extreme right) produces brine at an intermediate salinity, part of which is bled out and introduced as the make-up feed for the second stage and so on. The brine exiting the final stage is at the required high salinity, and part of this is bled out as the final brine. A multi-stage DCMD process for 70% overall recovery was studied by Ali et al. [7].

Options (a) and (b) are discontinuous/unsteady processes. Over each process cycle time, distillate is continuously removed and the remaining feed solution salinity increases until brine at the required high salinity is produced. At this point, the high-salinity brine is flushed out and the volume is refilled with new feed before the cycle is repeated. In batch recirculation, brine exiting the MD module is added back into a feed tank. The volume of solution in the tank reduces and concentration increases over time, until finally

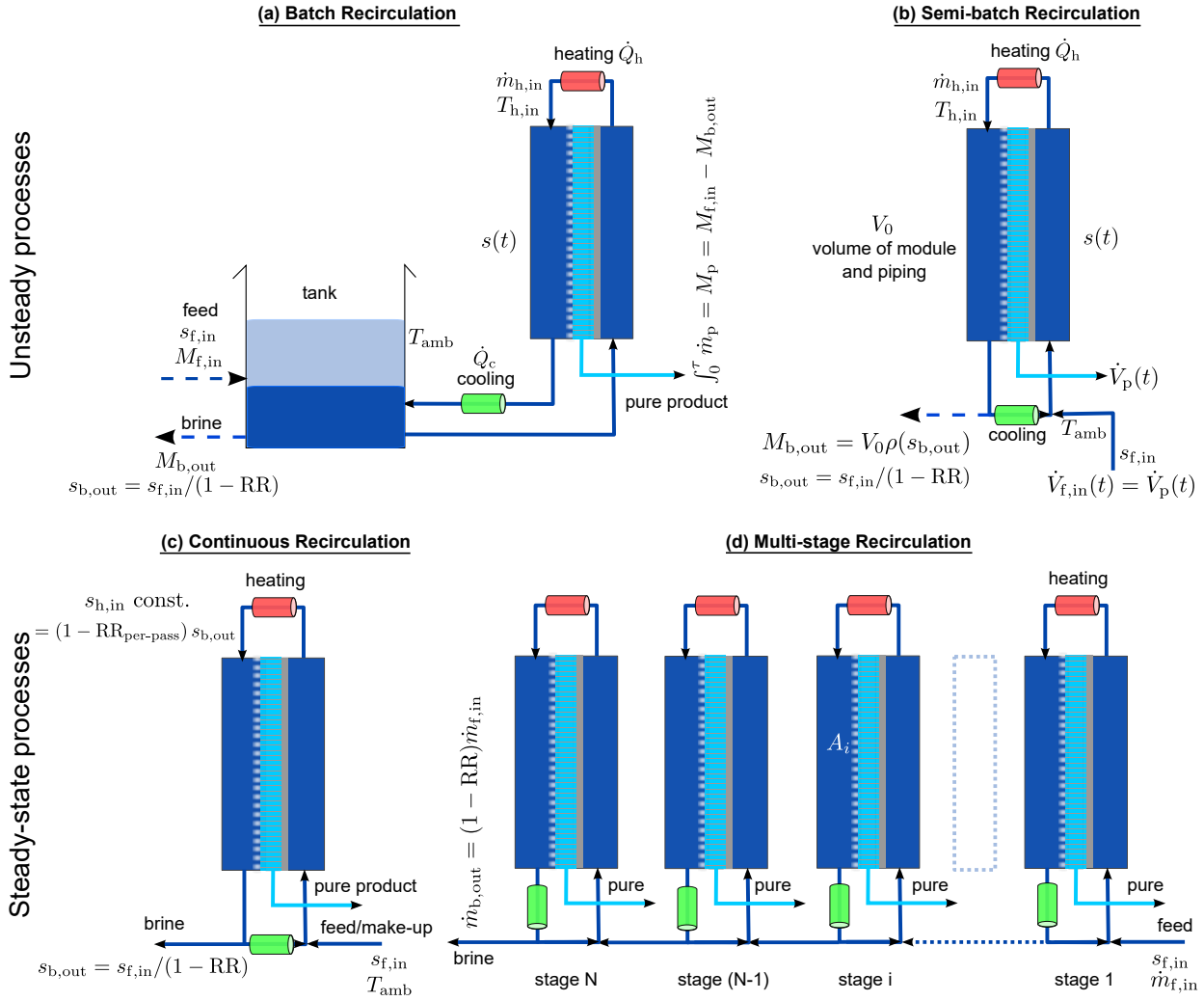

Figure 1: Schematic representation of batch, semibatch, continuous and multistage recirculation MD systems. These designs can be used to operate single-stage MD at an overall high recovery. Dotted arrows in Figs. (a), (b) indicate flows that occur only during the cycle change-over times. The subscript f denotes feed, b denotes brine, and p denotes permeate.

the concentration reaches $s_{b,out}$ (in our case 260 g/kg). At this point, brine is discharged and the tank is refilled with feed, as indicated by the dotted lines. The rate of permeate production ($\dot{m}_p$), as well as the heat transfer rate ($\dot{Q}_h$) would vary over the cycle time, as the feed to the MD module becomes more salty.

Most small scale bench-top experimental setups and small area implementations of MD, which have focused on achieving high flux (at high thermal energy consumption, operating at GOR < 1, where GOR is defined by Eq. (5) for any system) [8, 9, 10], recirculate the brine from the MD module back into the saline solution tank similar to what is illustrated in Fig. 1(a). Membrane distillation crystallization systems also have a recirculation loop similar to batch, where salts are allowed to precipitate out of solution before the feed is reintroduced into the MD module [11]. In some experimental devices, permeate may also be mixed back into the feed water tank periodically in order to test membrane performance at fixed feed salinity over an extended period of operation [12, 13].

Duong et al. [14] implemented batch recirculation for achieving high overall recovery (from 14.1 to 86.1 g/L) while also recovering the energy released during condensation for feed preheating. Recently, two studies have highlighted the energetic advantage of batch MD for high recovery applications. Bindels et al. [15] experimentally illustrated that the advantage of batch recirculation over continuous recirculation using the Aquastill AGMD modules. They found an energetic and time advantage of about 10% for batch over continuous recirculation while going from a feed salinity of 45 to 107 g/kg. Schwantes et al. [16] compared batch MD to MVC to show that MD in batch recirculation mode can be competitive with MVC for brine concentration from 70 – 250 g/kg, which is also the salinity range considered in the present study.

A semibatch recirculation design of RO has been commercially deployed [17]. Correspondingly, a semi-batch implementation of MD [Fig. 1b] is also evaluated in this study. In the semibatch process, the feed solution whose salinity increases over time is recirculated in a closed loop, without a variable volume tank. Since the volume of the piping is constant (V_0), to account for the mass lost into the permeate stream, feed water at $s_{f,in}$ is also continuously added into the loop. Since the rate of permeate production varies with time, the amount of feed water added into the semi-bath recirculation loop ($\dot{V}_{f,in}$) is also time varying. Eventually the salinity of water in the system would reach $s_{b,out}$. At this point, brine is flushed out by opening a valve and replaced by feed water.

Unlike MD, a single-pass RO process can reach high recovery ratios by increasing the feed pressure. The batch designs of RO therefore have to outperform single-pass RO in order to be competitive [18]. On the other hand, since single-pass MD at high recovery is not feasible, comparisons are made only amongst the recirculation designs.

1.3. Economic basis for comparison of high-recovery systems

The recirculation MD systems are compared based on their average energy efficiency (expressed as a non-dimensional inverse specific energy consumption or GOR) and water flux (J), which act as proxies for the operating and capital cost contributions to overall specific cost of water treatment. It has been shown

previously that the specific cost of water production can be expressed as $c_w \approx C_{heating}/GOR + C_{flux}/J$ (see Appendix A.1 in [19]; the factor $C_{heating}$ is a function of the unit cost of heat energy, and C_{flux} depends on the unit cost of system area). For brine concentration systems, the more relevant parameter is the specific cost per unit of incoming feed stream to be concentrated: $c_f = c_w \times RR$. All systems compared in this study have the same overall recovery ratio.

All the recirculation systems require additional cooling of the brine. Since brine is recirculated into the MD process on the preheating side, without additional cooling, coolant temperature would continuously increase causing flux to decline. The cooling load is proportional to the MD system's terminal temperature difference (TTD). In fact, the cooling load, $\dot{Q}_c = \dot{m}_f(1 - RR_{per\text{-}pass})c_p TTD_{cold}$, is quite close to the heating load $\dot{Q}_h = \dot{m}_f c_p TTD_{hot}$ since the TTD of a balanced MD system is similar at the hot and cold ends of the exchanger, the specific heat capacity c_p is not a strong function of temperature, and the flow rate difference is small ($RR_{per\text{-}pass}$ is small). As a result, the additional cooling term in the specific cost of brine concentration can be expressed similar to the thermal energy OpEx term as $C_{cooling}/GOR$, where where $C_{cooling}$ is a scaled cost of supplying coolant for a unit cooling load, accounting for the systematic differences in the cooling heat load $\dot{Q}_c$ compared to $\dot{Q}_h$ due to flow rate differences. Practically this factor ($C_{cooling}$) may be related to the energy consumption of the coolant fluid pump. The overall specific cost of brine concentration with MD can be written as:

$$\frac{c_f}{RR} \approx \frac{C_{flux}}{J} + \frac{C_{heating} + C_{cooling}}{GOR} \tag{3}$$

The different recirculation designs can be ranked by simultaneously comparing their GOR at fixed flux, or equivalently, flux at fixed GOR. Even though the membrane cost is the same, differences in other components (additional tank, control systems, or a staged design) can result in a variation in C_{flux} across different recirculation designs. This variation should be an additional consideration, especially if the difference in GOR and flux values is small.

1.4. Manuscript overview

In Section 2, the numerical methods used to evaluate the performance of the four recirculation systems are described. Batch, semibatch, and continuous recirculation are compared in Section 3 to show that batch always has a higher energy efficiency (GOR) at a given flux than semibatch which is in turn better than continuous recirculation. In Section 3.2, we compare multi-stage recirculation with batch to show that their overall performances are similar only when multi-stage employs a large number of stages.

The critical specific area (defined as the ratio of membrane area to feed inlet flow rate, operating above which results in a decline in both GOR and flux due to higher heat conduction losses through the membrane) changes over the cycle time of a batch MD process as the inlet salinity increases. Active control of the feed flow rate is required to prevent this counterproductive operation and is described in Section 4. The choice of optimal membrane thickness of batch MD is described in Section 5. Batch and continuous recirculation each with an optimized membrane thickness are compared.

2. Methodology

Swaminathan et al. [19, 20] showed previously that the overall performance of various single-stage MD configurations (air gap, permeate gap, and direct contact) is similar, if we account for differentiating variables such as effective membrane thickness, gap conductance and external heat exchanger area. Since the goal of this study is to compare various recirculation methods, we consider only the permeate/conductive gap MD configuration (CGMD) throughout. The conductance across the gap thickness is set at 10^4 W/m^2·K. A higher gap conductance results in improved GOR and flux, and would also more closely approximate the performance of DCMD (with a large external heat exchanger for energy recovery). This value of conductance was chosen since it can be practically achieved with a gap thickness of 0.5 mm and effective conductivity of 5 W/m·K. To make the comparisons fair across various recirculation modes, the same membrane material (based on permeability coefficient and effective thermal conductivity) is used, the overall recovery ratio is held constant ($s_\mathrm{f} = 70$ g/kg, $s_\mathrm{b} = 260$ g/kg), and same hot and cold inlet temperatures are imposed (85°C, 25°C). The full set of model assumptions and baseline system parameters are listed in Table 1.

Table 1: Baseline system parameters

Parameter	Value
Hot inlet temperature	85 °C
Cold inlet temperature	25 °C
Length L	6 m
Channel height	0.001 m
Inlet velocity $v_{\mathrm{f,in}}$	0.06 m/s
Membrane thickness δ_m	200 μm
Membrane permeability coefficient B_0	1.5×10^{-10} kg/m·s·Pa
Membrane overall thermal conductivity $k_{\mathrm{eff,m}}$	0.062 W/m·K
Salinity of feed, brine $s_\mathrm{f}, s_\mathrm{b}$	70, 260 g/kg

The thermodynamic and physico-chemical properties of the feed solution are approximations based on a pure sodium chloride solution. The dependence of conductivity (k) and viscosity (μ) on salinity are obtained as a curve fits based on reported data [21]. These fits are described in Appendix A. A correlation for Nusselt number in spacer filled channels is adapted from [22]: $Nu = 0.162 Re^{0.656} Pr^{0.333}$. The channel heat transfer coefficient can then be obtained as $h = (k/d_\mathrm{h}) \times Nu$, where d_h is the hydraulic diameter of the channel. Since both Re and Pr change with increasing feed salinity, changes in channel heat transfer coefficient over the cycle time of the process are accounted for. The increase in channel heat transfer coefficient at higher feed velocity is also captured.

The overall performance of the batch process is a function of system performance at each intermediate salinity from 70 to 260 g/kg. As a result, each evaluation of batch performance requires runs of the steady-

state model at various salinity levels. A modified ε-NTU method applicable to MD was developed in [20], to evaluate exchanger effectiveness (ε, which quantifies the extent of feed preheating) and MD thermal efficiency η (and hence GOR and flux) based on just the channel inlet conditions and dimensions, and total membrane area and properties, without having to solve for the local heat and mass transfer everywhere within the system. Plots comparing the results from this simplified HX model with results of a discretized model of MD solving for mass and energy conservation at each computational cell are included in Appendix A, Fig. A.12. Results from the full discretized MD model were previously validated against experimental data from pilot MD modules up to high feed salinity [19]. The average deviation in GOR and flux between the two models is only about 4%. The simplified HX model successfully captures key aspects of high salinity operation such as the existence of a critical feed flow rate. This simplified HX analogy model is therefore used in this study throughout to expedite calculations. Further model details are included in Appendix A.

2.1. Continuous Recirculation

The GOR and flux of continuous recirculation is the easiest to evaluate since it operates under steady state. The salinity at the MD module inlet is fixed in time such that $s_{\mathrm{h,in}}/(1-\mathrm{RR}_{\text{per-pass}}) = s_{\mathrm{b,out}}$. At the steady state condition, the feed salinity at the MD module inlet is close to the brine salinity because of MD's low recovery. For example, concentrating from 70 g/kg to 260 g/kg requires $s_{\mathrm{h,in}} \approx 245$–$250$ g/kg. Mixing of the makeup stream (e.g., 70 g/kg) with the recirculated brine stream (e.g., 260 g/kg) to form the feed stream (e.g., 245 g/kg) generates entropy and results in lower energy efficiency. Practically, the flux and GOR of continuous recirculation depends only on the final brine salinity and is independent of the feed salinity.

2.2. Continuous multistage recirculation

The performance of multistage MD is evaluated iteratively by solving the stages in sequence. The make-up feed salinity to the first stage is fixed at 70 g/kg. If a flow rate of the make-up feed to the first stage is chosen, the salinity and mass flow rate of the brine bleed from the first stage can be evaluated. These values act as inputs to the second stage, and so on. If the final stage brine salinity is higher than the required value of 260 g/kg, the original guess value of make up stream flow rate is increased. In this manner, iteratively the required overall RR can be achieved in the multistage system.

An additional variable involved in the design of multistage recirculation process is the fraction of the total membrane area allotted to each stage. The effect of area distribution is evaluated for a 2-stage system. Also, recirculation speed, channel length, and membrane thickness can be modified independently for each stage, but such an optimization is beyond the scope of this study.

2.3. Batch

The evaluation of batch and semibatch system performance is more complicated due to their transient operation. Over the cycle time of the process, the feed inlet to the MD module starts at 70 g/kg and goes

up all the way to saturation. As a result, the average flux over the cycle time (τ) has to be evaluated as a time average:

$$\overline{J} = \frac{\int_0^\tau J(t)\,dt}{\int_0^\tau dt} \tag{4}$$

$$\overline{\mathrm{GOR}} = h_{\mathrm{fg}} \frac{\int_0^\tau J(t) A\,dt}{\int_0^\tau \dot{Q}_{\mathrm{h}}(t)\,dt} \tag{5}$$

If the external feed tank is large enough, the rate of salinity change is slow. As a result, instantaneous performance is accurately represented by the steady-state MD model evaluated at instantaneous module inlet conditions. The flux and rate of heat addition at time t can therefore be evaluated using the steady state MD model if the salinity entering the module $s_{\mathrm{h,in}}(t)$ is known. Applying total mass and salt mass conservation to the feed solution (with no salt passage through the MD membrane):

$$\frac{dM}{dt} = -JA_{\mathrm{m}} \tag{6}$$

$$M(t)s(t) = M_{\mathrm{f}} s_{\mathrm{f}} \tag{7}$$

where M_{f} is the total mass of feed solution at the beginning of the batch cycle, and s_{f} is the original feed salinity. A_{m} is the membrane area.

Differentiating Eq. 7 with respect to t and substituting Eq. 6, the differential time required to achieve a small ds change in salinity of the system can be evaluated as:

$$dt_{\mathrm{batch}} = \frac{M_{\mathrm{f}} s_{\mathrm{f}}}{s^2 J(s) A_{\mathrm{m}}} ds \tag{8}$$

Observe that a smaller time increment is required for the same magnitude of change in solution salinity, as the feed salinity increases (assuming that the flux $J(s)$ does not decrease drastically). The total cycle time τ can be evaluated as the time that the system takes to go from s_{f} to s_{b}:

$$\tau_{\mathrm{batch}} = \int_0^{\tau_{\mathrm{batch}}} dt_{\mathrm{batch}} = \int_{s_{\mathrm{f}}}^{s_{\mathrm{b}}} \frac{M_{\mathrm{f}} s_{\mathrm{f}}}{s^2 J(s) A_{\mathrm{m}}} ds \tag{9}$$

The steady-state performance is evaluated at 50 intermediate salinity levels between 70 g/kg and 260 g/kg. At each of these values of s, $J(s)$ and $\dot{Q}_h(s)$ are obtained. Equation 9 is numerically integrated, plugging in these values of $J(s)$ to evaluate the total productive cycle time of the batch process, τ_{batch}.

Equation 8 can be plugged into Eqs. 4 and 5 to change the variable of integration to s. The limits of the integration then become s_{f} and s_{b}. The initial mass of feed M_{f} cancels between the numerator and denominator, and hence the result is independent of the tank size. A large tank is assumed so that the quasi-steady approximation made by using the steady-state MD model for instantaneous performance evaluation holds, and also so that the effects of transients in between cycles can be ignored.

2.4. Semibatch

In semibatch MD, the volume of the recirculation loop (V_0) is constant. As pure permeate is produced, fresh feed water is mixed into the loop to maintain the volume. Conservation of total mass and salt mass applied to the recirculation loop yields:

$$\frac{d(\rho V_0)}{dt} = V_0 \frac{d\rho}{dt} = \dot{m}_\mathrm{f} - JA_\mathrm{m} \tag{10}$$

$$\frac{d(\rho V_0 s)}{dt} = V_0 s \frac{d\rho}{dt} + V_0 \rho \frac{ds}{dt} = \dot{m}_\mathrm{f} s_\mathrm{f} \tag{11}$$

Approximating density as a linear function of salinity for NaCl solutions, $\rho(s) = \rho_\mathrm{pw} + \alpha s$, where s is in g/kg, $\alpha = 0.7261$ (kg/m^3)/(g/kg), we can rearrange the equations to get

$$dt_\mathrm{sb} = \frac{V_0(\rho_\mathrm{pw} + 2\alpha s - \alpha s_\mathrm{f})}{J(s) A_\mathrm{m} s_\mathrm{f}} \tag{12}$$

The rest of the steps in the evaluation are similar to the case of batch operation. Similar to batch operation, overall average GOR and flux are independent of the value of V_0.

2.5. Other assumptions

2.5.1. Cycle reset time

Some additional assumptions are inherent in the calculations above. For batch and semibatch cycles, the productive time of each cycle is considered to be approximately equal to the total cycle time neglecting the change-over time between cycles (when the brine is flushed out and fresh feed is refilled into the module). In other words, the time for cycle-reset is considered to be very small. One way to achieve this is shown in Fig. 2, by using an additional feed storage tank. At the end of one productive cycle-time, a valve can be actuated to draw fresh feed from the second feed tank. Initially, while highly saline brine is still being pushed out of the membrane channels, the brine will still be emptied into the first tank. Once all the brine is pushed out, the output from the module is also directed to the second tank. At this point, brine can be emptied from the first tank and fresh feed can be refilled. In this manner, the cycle reset time can be reduced.

In the case of semibatch MD, valves can be used to simultaneously push brine out and refill the module and pipes with fresh feed, to reduce the cycle change-over time.

2.5.2. Process startup

In all the comparisons, the energy associated with initial system start-up, i.e. providing the energy to heat up parts of the module up the top temperature of 85 °C is neglected, since the process is considered to operate repeatedly over several cycles or at steady state for a long duration. Similarly for continuous and multistage recirculation, the initial start-up and the energy associated with increasing the recirculated stream salinity from 70 g/kg to the operating salinity of 245 g/kg is neglected, assuming that steady state operation continues for a long duration.

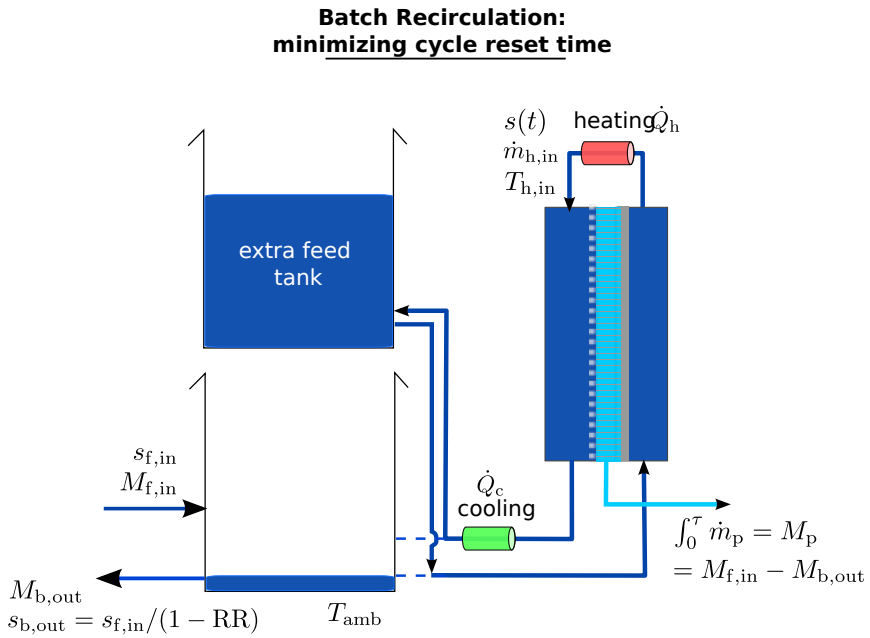

Figure 2: One way to reduce the cycle reset time between productive batch cycles using an extra feed tank.

2.5.3. Additional effects of high salinity

The effects of high salinity operation are a strong function of the composition of the feed stream. In addition to affecting the thermophysical properties of the feed and therefore the channel heat transfer coefficients, the composition also dictates whether some salts get supersaturated and form a scale on the membrane surface. While a large tank has been considered in this study to simplify the calculations neglecting initial and final transients, the overall residence time of high salinity water in the system increases with an increase in tank size [23]. Hence, from a practical fouling prevention standpoint, a smaller feed tank may be preferred if the feed composition has a high fouling tendency.

3. Comparison of recirculation systems

3.1. Comparing batch, semibatch and continuous recirculation

A single stage MD process can be designed to operate either at high flux and low energy efficiency or low flux and high GOR depending on the system size relative to feed flow rate (expressed non-dimensionally as NTU, or number of transfer units). The dimensionless specific system area is defined as:

$$\mathrm{NTU} = \frac{A}{\dot{m}_{\mathrm{f,in}}} \cdot \frac{U}{c_{\mathrm{p}}} \tag{13}$$

where U is the overall heat transfer coefficient between the hot feed and cold preheat streams.

At large NTU, the exchanger effectiveness (ε) is higher, i.e., the cold stream would get preheated more and leave closer to the hot inlet temperature. While this results in a higher energy efficiency (due to lower $\dot{Q}_{\mathrm{h}}$), the driving temperature difference for water production will be low throughout the module length and

hence flux will be low. Designing at a low NTU has the opposite effect and helps achieve a high flux, at the expense of lower energy efficiency.

Similar to single-pass MD, recirculation systems can also be designed with a long or short module length relative to the feed inlet velocity. Figure 3 shows the GOR and flux performance of batch, semibatch and continuous recirculation systems at a range of module lengths: $L = 1.8$–6 m. The ideal module length for each design (or equivalently, the ideal combination of GOR and flux at which the system should be designed) is a function of the relative unit costs of system area (CapEx) and heat energy and cooling (OpEx), i.e. $C_{\text{flux}}/(C_{\text{heating}} + C_{\text{cooling}})$. The unit cost of heat energy varies with plant location, and the cost of system area can decrease with larger scale production capacity. Without considering specific cost numbers, recirculation designs can be compared generally based on Fig. 3. Notice that at any given value of flux, GOR of batch is much higher than that of semibatch, which in turn is higher than continuous recirculation. As a result, we can conclude that batch outperforms semibatch and continuous recirculation designs.

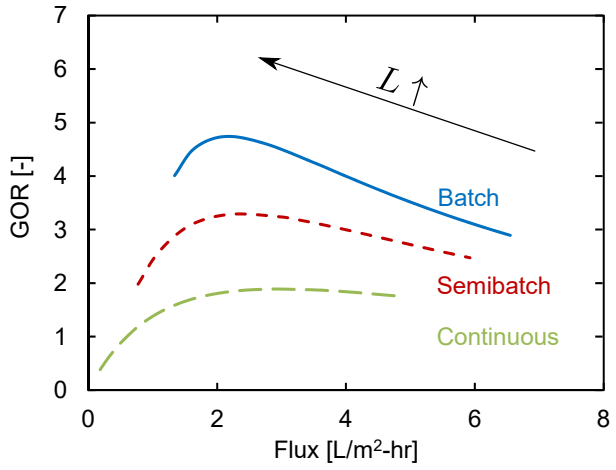

Figure 3: GOR-flux performance curves of batch, semibatch and continuous recirculation systems by varying system size ($L = 1.8$–6 m). Batch performs better than semibatch MD, which in turn outperforms continuous recirculation. $\delta_{\text{m}} = 200$ μm, $v_{\text{f,in}} = 6$ cm/s.

Note that for all three alternatives, both GOR and flux start to decrease beyond a critical system size. We will revisit this issue in Section 4.

3.1.1. Batch spends more time at lower salinities

All three configurations desalinate water over the same salinity range producing a brine at 260 g/kg from feed at 70 g/kg. The insets in Figure 4 show the flux and heat input rate as a function of feed salinity over this range. As the inlet salinity increases, the resistance to vapor transport within the MD module rises, and correspondingly, J decreases. Since the feed preheating is reduced, $\dot{Q}_{\text{h}}$ increases. As a result, both instantaneous flux and GOR decrease with an increase in feed salinity.

The relative amount of time each system spends at various salinities is different, and this causes the

difference in overall performance. Figure 4 shows J and $\dot{Q}_\mathrm{h}$ in the batch, semibatch and continuous recirculation systems over non-dimensional cycle time (t/τ). Since continuous recirculation is a steady-state process, the curve is flat with time. For batch and semibatch, non-dimensional time is evaluated relative to their own cycle times. Note that since batch spends relatively larger fraction of time at lower salinity (as a consequence of Eqs. 8, 12), its time-averaged flux is higher and averaged heat input rate is lower than those of the other configurations.

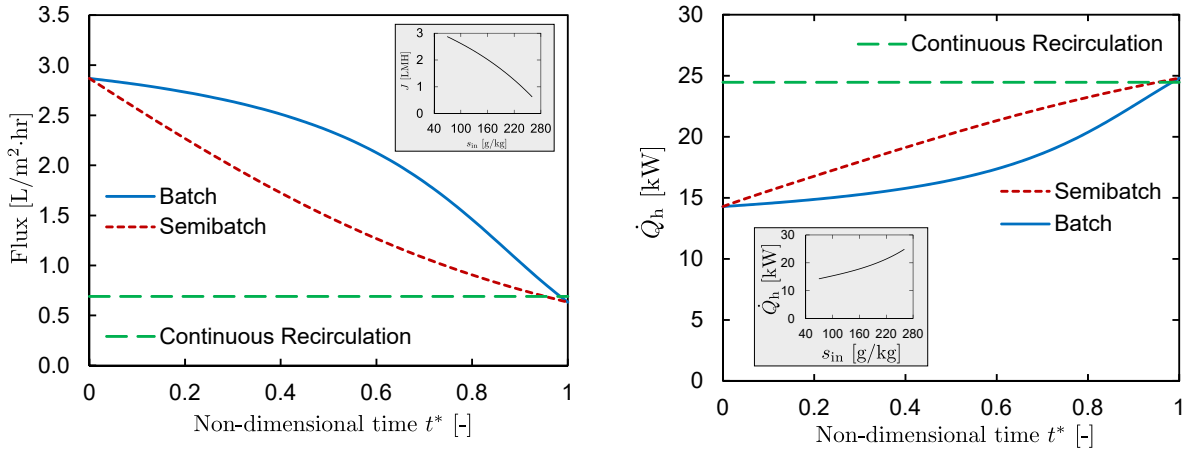

(a) Flux over the process cycle time.

(b) The heater input over the process cycle time.

Figure 4: Flux and heat supply over the cycle time of the batch and semibatch processes. Continuous recirculation, which is a steady process is also shown for contrast. $L = 4.8$ m, $v_\mathrm{in} = 0.06$ m/s, $\delta_\mathrm{m} = 200$ μm. The dependence of flux and heat supply on feed inlet salinity is the same irrespective of recirculation mode and is shown in the insets.

3.1.2. Advantage of batch recirculation is more pronounced at high salinity

The comparison between batch, semibatch, and continuous recirculation is a function of the range of feed salinities that are handled by the system. For the same value of overall recovery ratio, the range of salinity treated is much larger when the feed salinity is higher. For a 72% recovery process from 5 g/kg to 18.6 g/kg, the change in GOR and flux over this salinity range is so small that all three designs perform essentially the same. At higher salinity, however, the difference is more significant (Fig. 5).

Similarly, for AGMD or a thick CGMD membrane system that is operated at high flux, the change in performance with changes in feed salinity is small. As a result, once again, the difference between batch, semibatch, and continuous recirculation would be small. In such cases, for simplicity, a continuous recirculation system may be preferable.

3.2. Multistage recirculation

The GOR and flux performance of multistage recirculation (Fig. 1(d)) with increasing number of stages is compared against continuous and batch recirculation in Figure 6. At one stage, the system is equivalent to a continuous recirculation design. As the number of stages is increased, the number of intermediate salinity

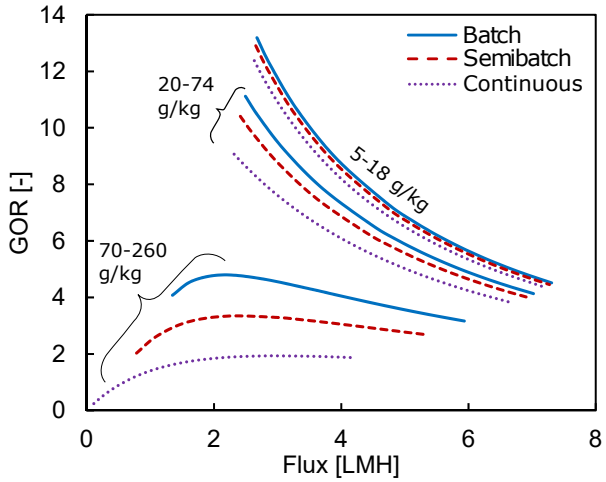

Figure 5: The GOR-flux performance is compared between the three recirculation designs at various values of feed inlet salinity (s_f =5,20, and 70 g/kg), at the same overall RR (= 0.72). L = 2–6 m, δ_m = 200 μm, v_{in} = 0.06 m/s. The relative benefit of operating in batch mode is higher at high inlet salinity.

levels at which MD is operated increases. In Fig. 6, the total membrane area is divided equally among the stages, for each value of N_{stages}.

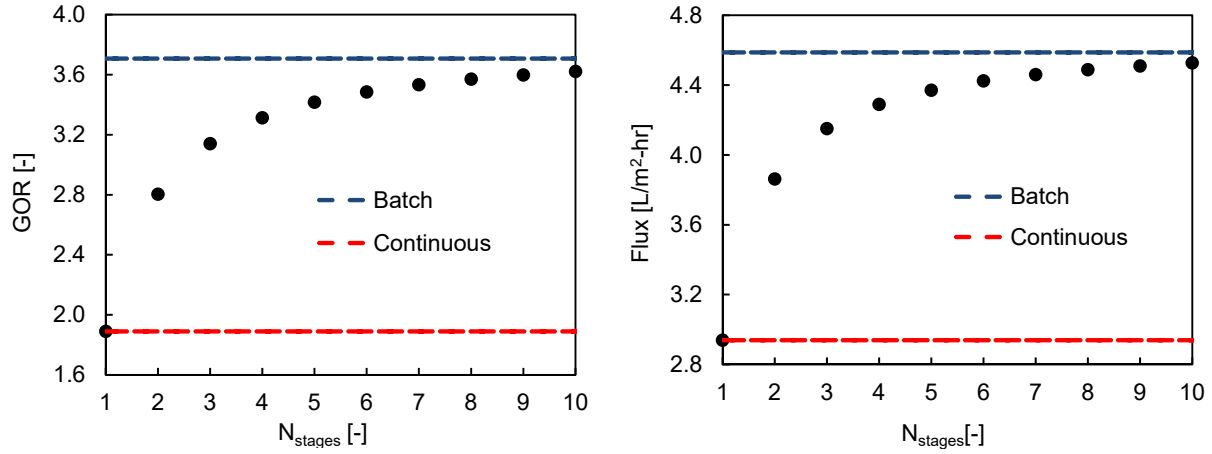

(a) GOR as a function of number of stages.

(b) Flux as a function of number of stages.

Figure 6: GOR and flux vs. N_{stages} for multi-stage recirculation. L = 2.57 m and $v_{f,in}$ = 0.06 m/s for all stages and for the batch system. Total area in multi-stage recirculation is divided equally between stages by choosing equal module width in each stage. Batch and continuous recirculation are shown for comparison.

Both GOR and flux of multistage recirculation approach that of a batch system as the number of stages increases. This is because multistage recirculation performs in space what a batch system does in time, i.e., it treats water at a range of feed salinity levels between 70 and 260 g/kg, unlike single-stage continuous recirculation. While a large number of stages is required to approach batch-like performance, the advantage of adding an additional stage is much higher at a low number of stages.

Although multistage recirculation is a steady state process that can achieve batch-like performance, the number of heaters and other components scales with N_{stages} and would likely make it unattractive compared to batch recirculation.

The effect of area distribution among the various stages is considered for the simplest case of a two-stage device in Fig. 7. Since L and v are held constant at the same values as Fig. 6, the relative area between the stages is adjusted by changing the channel width values. With two stages, the optimized arrangement places about 66% of the total area into the first stage. Just as a batch process spends more time at lower salinity levels, a larger area of an initial stage results in a higher fraction of area investment for desalination of the feed at lower salinity.

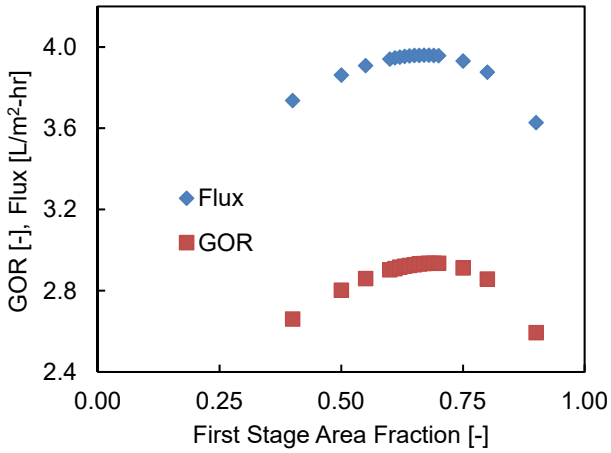

Figure 7: GOR and flux of a two-stage recirculation system as a function of fraction of total membrane area alloted to the first stage.

Note that in spite of these optimizations, a multistage MD process can only approach the performance of batch RO with a large number of stages. Practically, the cost of implementing high N_{stages} would increase due to the larger number of pipe components for the same total membrane area, and hence C_{flux} for a multistage design would be higher even though the membrane unit cost is the same. As a result, we can conclude that batch operation is the best alternative for brine concentration with MD to achieve high overall GOR and flux.

4. System operation: Adjust feed flow rate over batch cycle time

At high feed salinity, vapor pressure depression of the feed lowers the vapor transfer driving force, even as the driving force for heat conduction loss through the membrane remains unaffected. As a result, beyond a certain specific area (or NTU^{crit}) at a fixed feed salinity, heat conduction loss ($\dot{Q}_{\text{m,cond}}$) begins to dominate over vapor transport (as the temperature difference across the membrane approaches boiling point elevation), resulting in a lowering of both GOR and flux with further increase in system specific area.

This effect is practically important and has been observed experimentally. Hitsov et al. [24] report measured GOR and flux with a 7.2 m^2 membrane area for AGMD and DCMD configurations while varying feed inlet flow rate. At 200 g/L, the DCMD system shows a decline in both GOR and flux when the feed inlet flow rate is reduced from 1000 L/hr to 500 L/hr for both 50 °C and 70 °C module top temperatures. This indicates that the critical flow rate is above 500 L/hr at 200 g/L. The reported data also shows that the critical flow rate is below 500 L/hr at feed salinity values of 60 g/L and 100 g/L. If this module was being operated in batch mode at feed inlet flow rate of 500 L/hr, for feed salinities $s \leq 100$ g/L, increasing the feed flow rate upward from 500 L/hr results in an increase in flux at the expense of a reduced GOR (which may or may not be advantageous depending on the cost of heat energy). Starting somewhere between 100–200 g/L, increasing feed flow rate up from 500 L/hr results in simultaneous improvement of GOR and flux, and hence would be advantageous irrespective of the value of $C_{\text{flux}}/(C_{\text{heating}} + C_{\text{cooling}})$. Thus, we can see the practical value of increasing feed velocity during the cycle time of a batch process as the inlet salinity increases, to avoid excessive heat conduction losses and hence low operating flux and GOR levels. Similarly, data from PGMD modules with 10 m^2 membrane area in Winter et al. [25] show critical flow rates of around 200 kg/hr for $s = 50$ and 75 g/kg.

The above studies found a critical flow rate, below which the fixed membrane area system must not be operated. Equivalently, this information can be expressed as a critical specific area above which the system should not be operated. Swaminathan et al. [19] derived an expression for NTU^{crit} as a function of membrane and channel heat transfer properties and feed salinity. NTU^{crit} is higher at low salinity, high $B_0/k_{\text{eff,m}}$ and when the channel heat transfer coefficient is high. Figure 8 shows that this critical specific area is a strong function of feed salinity and decreases rapidly with increase in s. Equivalently, the critical flow rate for a fixed area system would increase with increase in feed salinity.

Unlike continuous MD, the critical specific area (or NTU^{crit})of batch MD increases over the cycle time of the process as the feed salinity increases (as indicated by the x-coordinates of the peaks of the curves in Fig. 8. As a result, avoiding the counterproductive operating regime only at the beginning of the process (e.g., operating at 2 m^2/(L/min)) is not sufficient. Throughout the cycle time, it must ideally be ensured that $\text{NTU} \leq \text{NTU}^{\text{crit}}$.

Over the course of the cycle, if the feed velocity is kept constant, it is possible to move from an allowable operating condition (i.e., to the left of the red dots) to the undesirable areas of the GOR-specific area curve (to the right of the red dots), such as in the case of the red arrow shown in Fig. 8. One such operating condition (for $\delta_{\text{m}} = 200$ μm, $L = 4.8$ m) is operating at constant velocity $v = 6$ cm/s, throughout the cycle time. The corresponding flux and $\dot{Q}_{\text{h}}$ profiles as a function of non-dimensional time are shown as dotted lines in Fig. 9. The operating condition transitions to the counterproductive regime starting at about 180 g/kg. This transition salinity is a function of system size, channel heat transfer coefficients and membrane properties. A system with a small membrane area, a thick membrane, or higher heat transfer coefficient may not enter counterproductive operating conditions even if velocity is held constant throughout the cycle. The

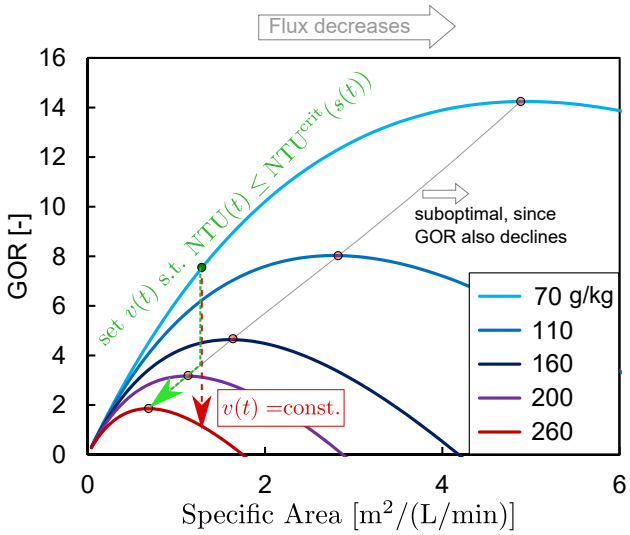

Figure 8: Effect of specific area on GOR at a range of feed salinity values. Flux always decreases with increase in specific area. Operating at specific area > critical specific area (corresponding to the peaks of the curves) results in a decline in GOR also. Specific area is defined here as the membrane area divided by the inlet volume flow rate of hot feed.

overall GOR for this case, operating at constant velocity, is 4.8 and flux is 2.13 L/m^2·hr.

In a real system, NTU can be inferred based on inlet and outlet temperatures, and can be compared against the predicted NTU$^{\text{crit}}$, which is a function of feed inlet salinity. During operation, the feed velocity can be increased as inlet salinity increases, to ensure operation below NTU$^{\text{crit}}$. The corresponding flux and heat input rates for such operation are shown by the solid lines in Fig. 9. Towards the end of the cycle time, the inlet velocity is increased from 6 cm/s to about 12 cm/s (as shown in the inset). This leads to an improvement in both overall GOR and flux to 5.2 and 2.47 L/m^2·hr.

The reason for the deviation between the dotted and solid lines even before $t^* = 0.8$ is that the cycle time is different for the two cases. The system with velocity control operates at higher flux towards the end of the cycle and hence spends lesser time at high salinity. Lower time at high salinity is one of the reasons for improved overall performance with active control of feed velocity during the process cycle time. Note that though both J and $\dot{Q}_{\text{h}}$ increase relative to the case of constant velocity, the flux towards the end the cycle increases by about a factor of 5, whereas heat input rate increases by only a factor of about 3. As a result, GOR is also improved by this velocity control scheme.

Note that when increasing $v(t)$ in real systems, the increase in pressure drop must be also considered. If the pressure drop increases significantly, the pressure in the feed channel can exceed LEP, leading to membrane failure.

Figure 10 shows the advantage of adjusting instantaneous v such that the NTU $\leq$ NTU$^{\text{crit}}$ for a range of system lengths (L = 1.8–6 m), on a GOR-flux performance plot. The dotted line is reproduced from Fig. 3, whereas the solid lines represents the new improved performance with velocity control. Velocity control is not necessary for short modules (operating at larger flux). In order to show that the improved GOR is

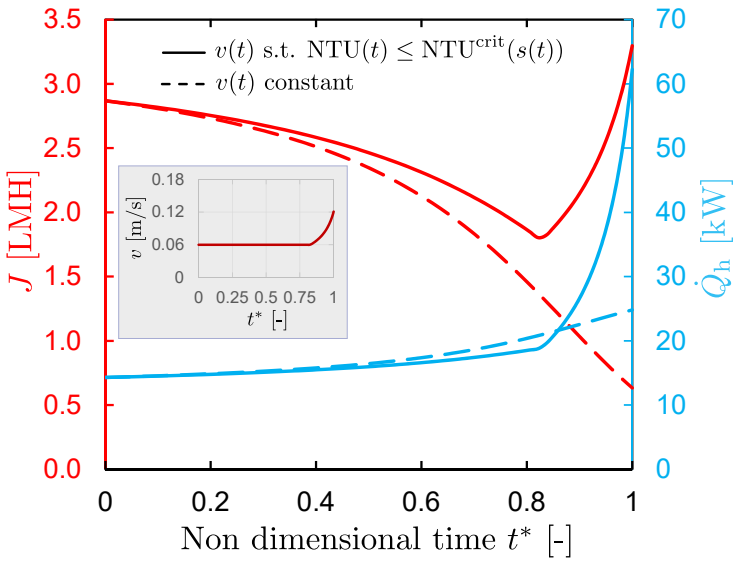

Figure 9: Flux and heat supply over the cycle times of the process. Non-optimal condition is avoided by adjusting $v(t)$ such that $\mathrm{NTU}(t) \leq \mathrm{NTU}^{\mathrm{crit}}(s(t))$. Inset: Velocity profile over the cycle time to ensure $\mathrm{NTU} \leq \mathrm{NTU}^{\mathrm{crit}}$.

not due to the increased heat transfer coefficient at elevated velocities, the performance at a constant high velocity of 15.2 cm/s is plotted in red. While a constant high velocity is better (achieves higher GOR at the same flux compared to the other curves), its maximum GOR with a module length of $L = 6$ m indicated by the left most point of the red curve is much lower than what is achieved with active velocity control. This is because a constantly high velocity reduces NTU throughout the cycle time, and results in higher flux at the expense of lower GOR. In order to achieve a higher GOR than 6 with the high velocity system, a much longer module length than 6 m would be required, which would again be limited by pressure drop considerations.

5. System design: Optimal membrane thickness and comparison with continuous recirculation

All the previous analysis was performed at one value of the membrane thickness, $\delta_{\mathrm{m}} = 200$ μm. Here, we relax this constraint, as we are free to pick any membrane thickness at the design stage. Thicker membranes enable reaching higher GOR values at high salinity and large system size, by reducing the effect of heat conduction losses, but result in a poorer GOR when operating at small system size or high operating flux [19]. This trend holds true when performance is averaged over the cycle time in the case of batch MD as well. Overall, the GOR-flux performance curves for all the membrane thicknesses can be plotted together and the upper limit profile can be identified as the best case GOR-flux operating condition for the given membrane $B_0/k_{\mathrm{eff,m}}$ and h_{ch}.

At each module length and operating flux, the optimal membrane thickness for a continuous recirculation system can be numerically evaluated. GOR vs. flux performance of continuous recirculation with optimized membrane thickness is plotted as a dotted line in Fig. 11a. The batch MD curve is approximated by plotting

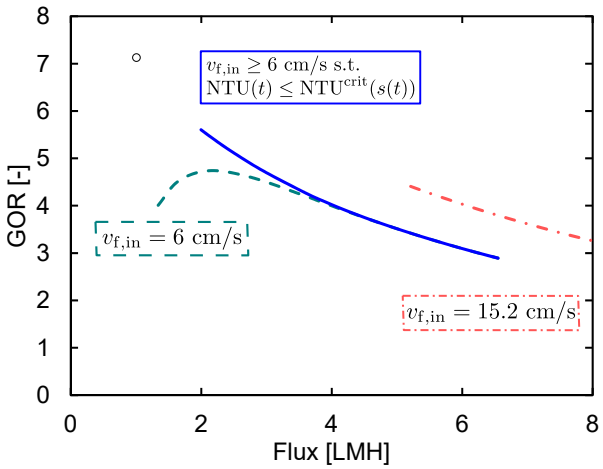

Figure 10: Advantage of adjusting $v(t)$ such that $\mathrm{NTU} \leq \mathrm{NTU}^{crit}$. Higher GOR and flux can be obtained by actively controlling v to avoid counterproductive conditions. Operating at a constant high v with the same membrane length would have a lower GOR, due to NTU being lower. $L = 1.8$–6 m, $\delta_m = 200$ μm.

performance curves at discrete values of δ_m and choosing a portion each curve to obtain an overall maximum GOR vs. flux curve (see e.g., Fig. B.13 in 5). The GOR of a batch system is around 2 times higher than that of a continuous recirculation system over a range of flux values.

The corresponding optimal membrane thickness for batch and continuous recirculation are shown in Fig. 11b. At high flux and low GOR operation (small module length), the optimal membrane thickness is lower for both designs, since the driving temperature difference across the membrane is large compared to boiling point elevation and hence vapor transport dominates over heat conduction loses through the membrane. Since batch MD operates at a range of salinities much lower than continuous recirculation, its optimal membrane thickness at the same overall flux is about one half that of continuous recirculation.

While very high GOR is possible with batch MD (using thick membranes), the module length for such designs is also very large (for example, the module length corresponding to the 600 micron membrane thickness operating at a GOR of more than 7.5 is about 18 m). Also, the velocity would have to be increased towards the end of the cycle time to about 15 cm/s in this case. Channel pressure drop would therefore limit the practically feasible limits of high GOR operation with batch MD with optimized membrane thickness. Membrane thickness optimization in batch systems without velocity control is considered in Appendix B.

A multistage MD system can be designed with a thin membrane in the initial stages when the feed salinity is low, and progressively thicker membranes at subsequent stages which treat more salty water. This would be equivalent to using conductive gap or direct contact MD at the low salinity stages, and air gap MD at the later stages operating at high salinity to reduce heat conduction loss. While such a design shows promise for improvement of GOR and flux, a detailed analysis of such systems is beyond the scope of the present manuscript.

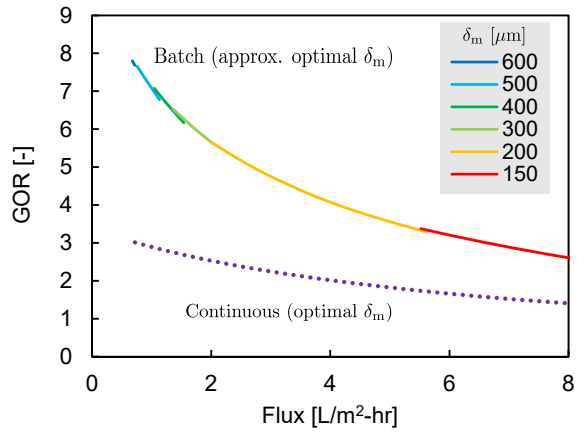

(a) Comparison of GOR-flux operating curves of batch and continuous recirculation MD with optimized δ_m. At each δ_m, the feed velocity is allowed to vary to vary avoid NTU $>$ NTU^{crit} as described in Section 4.

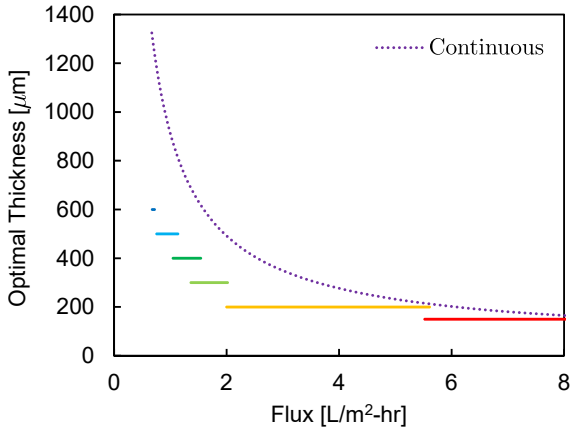

(b) Optimal membrane thickness of batch is indicated by the solid lines and optimal membrane thickness of continuous recirculation MD is indicated by the dotted line. Only a discrete set of δ_m values were considered for the batch operation.

Figure 11: Optimizing membrane thickness when designing batch and continuous recirculation MD.

6. Concluding remarks

Batch operation achieves higher GOR at a given flux than semibatch and continuous recirculation because the batch system operates at lower feed salinity levels for a larger fraction of its total cycle time. Continuous multistage recirculation can achieve performance close to that of batch only with a large number of stages. A multistage system may further be optimized by unequally splitting the total membrane area among the various stages. While multistage with large number of stages approaches the performance of batch, high N_{stages} results in added complexity and therefore higher capital cost per unit system area. Batch recirculation is therefore established as the best alternative among the four recirculation methods considered, for achieving energy efficient and high flux brine concentration. The relative advantage of batch over the other designs is most signficant for high inlet feed salinity and high RR. The change-over time between operating cycles of the batch process must be minimized for efficient use of the available membrane area.

To maintain good GOR-flux performance throughout the batch process cycle time, the feed velocity, v, may have to be increased such that the non-dimensional system specific area NTU is lesser than or equal to the critical value, NTU^{crit}. This ensures that heat conduction losses do not dominate towards the end of the cycle time as the feed salinity increases.

Batch MD can achieve about two times higher GOR, at the same value of flux, compared to a continuous recirculation system, when an optimal membrane thickness is chosen in both cases. The optimal membrane is thin in the case of short modules operating at high flux and thicker for long modules aimed at achieving high GOR. The optimal thickness in the case of batch MD is about one half the optimal thickness of a continuous

recirculation system. While very high GOR (at correspondingly low flux) is possible with batch MD using a thick membrane, it requires a long module length. Therefore, in practice pressure drop considerations will limit the maximum GOR achievable.

Acknowledgments

Jaichander Swaminathan thanks the Tata Center for Technology and Design at MIT for funding this work. The authors also thank Hyung Won Chung and David Warsinger for useful discussions.

References

[1] E. Guillén-Burrieza, G. Zaragoza, S. Miralles-Cuevas, J. Blanco, Experimental evaluation of two pilot-scale membrane distillation modules used for solar desalination, Journal of Membrane Science 409-410 (2012) 264 – 275. doi:https://doi.org/10.1016/j.memsci.2012.03.063.
URL http://www.sciencedirect.com/science/article/pii/S0376738812002645

[2] A. Deshmukh, M. Elimelech, Understanding the impact of membrane properties and transport phenomena on the energetic performance of membrane distillation desalination, Journal of Membrane Science 539 (2017) 458–474. doi:https://doi.org/10.1016/j.memsci.2017.05.017.
URL http://www.sciencedirect.com/science/article/pii/S0376738817308323

[3] G. Guan, X. Yang, R. Wang, A. G. Fane, Evaluation of heat utilization in membrane distillation desalination system integrated with heat recovery, Desalination 366 (2015) 80–93. doi:10.1016/j.desal.2015.01.013.
URL http://linkinghub.elsevier.com/retrieve/pii/S0011916415000181

[4] N. Koeman-Stein, R. Creusen, M. Zijlstra, C. Groot, W. van den Broek, Membrane distillation of industrial cooling tower blowdown water, Water Resources and Industry 14 (2016) 11–17. doi:http://doi.org/10.1016/j.wri.2016.03.002.
URL http://www.sciencedirect.com/science/article/pii/S2212371716300051

[5] H. W. Chung, J. Swaminathan, D. M. Warsinger, J. H. Lienhard, Multistage vacuum membrane distillation (MSVMD) systems for high salinity applications, Journal of Membrane Science 497 (2016) 128–141. doi:10.1016/j.memsci.2015.09.009.
URL http://www.sciencedirect.com/science/article/pii/S0376738815301733

[6] O. R. Lokare, S. Tavakkoli, V. Khanna, R. D. Vidic, Importance of feed recirculation for the overall energy consumption in membrane distillation systems, Desalination 428 (2018) 250–254. doi:https://doi.org/10.1016/j.desal.2017.11.037.
URL http://www.sciencedirect.com/science/article/pii/S0011916417320325

[7] A. Ali, C. Quist-Jensen, F. Macedonio, E. Drioli, Optimization of module length for continuous direct contact membrane distillation process, Chemical Engineering and Processing: Process Intensification 110 (2016) 188–200. doi:http://doi.org/10.1016/j.cep.2016.10.014.
URL http://www.sciencedirect.com/science/article/pii/S0255270116305220

[8] D. Amaya-Vías, E. Nebot, J. A. López-Ramírez, Comparative studies of different membrane distillation configurations and membranes for potential use on board cruise vessels, Desalination 429 (2018) 44–51. doi:https://doi.org/10.1016/j.desal.2017.12.008.
URL http://www.sciencedirect.com/science/article/pii/S0011916417314121

[9] H. C. Duong, P. Cooper, B. Nelemans, T. Y. Cath, L. D. Nghiem, Optimising thermal efficiency of direct contact membrane distillation by brine recycling for small-scale seawater desalination, Desalination 374 (2015) 1–9. doi:https://doi.org/10.1016/j.desal.2015.07.009.
URL http://www.sciencedirect.com/science/article/pii/S0011916415300175

[10] E. Guillen-Burrieza, J. Blanco, G. Zaragoza, D.-C. Alarcn, P. Palenzuela, M. Ibarra, W. Gernjak, Experimental analysis of an air gap membrane distillation solar desalination pilot system, Journal of Membrane Science 379 (1) (2011) 386–396. doi:https://doi.org/10.1016/j.memsci.2011.06.009.
URL http://www.sciencedirect.com/science/article/pii/S0376738811004479

[11] C. M. Tun, A. G. Fane, J. T. Matheickal, R. Sheikholeslami, Membrane distillation crystallization of concentrated salts-flux and crystal formation, Journal of Membrane Science 257 (1-2) (2005) 144–155. doi:10.1016/j.memsci.2004.09.051.
URL http://linkinghub.elsevier.com/retrieve/pii/S0376738804008361

[12] D. M. Warsinger, E. W. Tow, J. Swaminathan, J. H. Lienhard, Theoretical framework for predicting inorganic fouling in membrane distillation and experimental validation with calcium sulfate, Journal of Membrane Science 528 (2017) 381–390. doi:https://doi.org/10.1016/j.memsci.2017.01.031.
URL http://www.sciencedirect.com/science/article/pii/S0376738817301916

[13] D. Singh, P. Prakash, K. K. Sirkar, Deoiled produced water treatment using direct-contact membrane distillation, Ind. Eng. Chem. Res. 52 (2013) 13439–13448. doi:10.1021/ie4015809.
URL http://pubs.acs.org/doi/full/10.1021/ie4015809

[14] H. C. Duong, A. R. Chivas, B. Nelemans, M. Duke, S. Gray, T. Y. Cath, L. D. Nghiem, Treatment of RO brine from CSG produced water by spiral-wound air gap membrane distillation: A pilot study, Desalination 366 (2015) 121–129. doi:http://doi.org/10.1016/j.desal.2014.10.026.
URL http://www.sciencedirect.com/science/article/pii/S0011916414005499

[15] M. Bindels, N. Brand, B. Nelemans, Modeling of semibatch air gap membrane distillation, Desalination 430 (2018) 98–106. doi:https://doi.org/10.1016/j.desal.2017.12.036.
URL http://www.sciencedirect.com/science/article/pii/S0011916417307257

[16] R. Schwantes, K. Chavan, D. Winter, C. Felsmann, J. Pfafferott, Techno-economic comparison of membrane distillation and MVC in a zero liquid discharge application, Desalination 428 (2018) 50–68. doi:https://doi.org/10.1016/j.desal.2017.11.026.
URL http://www.sciencedirect.com/science/article/pii/S0011916417313176

[17] R. L. Stover, Industrial and brackish water treatment with closed circuit reverse osmosis, Desalination and Water Treatment 51 (4–6) (2013) 1124–1130. arXiv:http://dx.doi.org/10.1080/19443994.

2012.699341, doi:10.1080/19443994.2012.699341.
URL http://dx.doi.org/10.1080/19443994.2012.699341

[18] J. Swaminathan, R. L. Stover, E. W. Tow, D. M. Warsinger, J. H. Lienhard, Effect of practical losses on optimal design of batch RO systems, in: Proceedings of IDA World Congress on Desalination and Water Reuse, Sao Paulo, Brazil, International Desalination Association, 2017, pp. IDA17WC–58334.
URL http://hdl.handle.net/1721.1/111971

[19] J. Swaminathan, H. W. Chung, D. M. Warsinger, J. H. Lienhard, Energy efficiency of membrane distillation up to high salinity: Evaluating critical system size and optimal membrane thickness, Applied Energy 211 (2018) 715–734. doi:https://doi.org/10.1016/j.apenergy.2017.11.043.
URL http://www.sciencedirect.com/science/article/pii/S0306261917316185

[20] J. Swaminathan, H. W. Chung, D. M. Warsinger, J. H. Lienhard, Membrane distillation model based on heat exchanger theory and configuration comparison, Applied Energy 184 (2016) 491–505. doi:http://dx.doi.org/10.1016/j.apenergy.2016.09.090.
URL http://www.sciencedirect.com/science/article/pii/S0306261916313927

[21] C. G.R., C. F., M. R., T. J., Physicothermal properties of aqueous sodium chloride solutions, Journal of Food Process Engineering 38 (3) 234–242. arXiv:https://onlinelibrary.wiley.com/doi/pdf/10.1111/jfpe.12160, doi:10.1111/jfpe.12160.
URL https://onlinelibrary.wiley.com/doi/abs/10.1111/jfpe.12160

[22] D. Winter, Membrane distillation: A thermodynamic, technological and economic analysis, Ph.D. thesis, University of Kaiserslautern, Germany (2015).
URL http://www.reiner-lemoine-stiftung.de/pdf/dissertationen/Dissertation-Winter.pdf

[23] D. M. Warsinger, E. W. Tow, L. A. Maswadeh, G. B. Connors, J. Swaminathan, J. H. Lienhard, Inorganic fouling mitigation by salinity cycling in batch reverse osmosis, Water Research 137 (2018) 384 – 394. doi:https://doi.org/10.1016/j.watres.2018.01.060.
URL http://www.sciencedirect.com/science/article/pii/S0043135418300745

[24] I. Hitsov, K. D. Sitter, C. Dotremont, P. Cauwenberg, I. Nopens, Full-scale validated air gap membrane distillation (agmd) model without calibration parameters, Journal of Membrane Science 533 (2017) 309 – 320. doi:http://doi.org/10.1016/j.memsci.2017.04.002.
URL http://www.sciencedirect.com/science/article/pii/S0376738816325170

[25] D. Winter, J. Koschikowski, M. Wieghaus, Desalination using membrane distillation: Experimental studies on full scale spiral wound modules, Journal of Membrane Science 375 (1-2) (2011) 104–112. doi:10.1016/j.memsci.2011.03.030.
URL http://linkinghub.elsevier.com/retrieve/pii/S0376738811002067

[26] E. K. Summers, H. A. Arafat, J. H. Lienhard, Energy efficiency comparison of single-stage membrane distillation (MD) desalination cycles in different configurations, Desalination 290 (2012) 54–66. doi:10.1016/j.desal.2012.01.004.
URL http://linkinghub.elsevier.com/retrieve/pii/S0011916412000264

Appendix A. Model details, comparisons

The discretized model of the MD process that iteratively solves for the local temperatures in the channels, as well as local pure vapor and heat conduction fluxes through the membrane have been described previously [26]. The effects of changes in salinity over the cycle time of the batch process are captured using the following equations as a function of molality (m in mol/kg-water) or salinity (s in g/kg). The parameters are evaluated the system average temperature of about 55 °C. Density and viscosity increase with salinity, whereas c_p and thermal conductivity decrease.

$$\begin{aligned}\rho =& 1028.58 + 38.23m - 1.043m^2\\ c_\mathrm{p} =& 4169 - 249.1m + 16.25m^2\\ \mu =& 2.239\times10^{-4}s^{0.2306}\\ k =& 0.6465 - 0.00581\times10^{-3}m - 0.000154\times10^{-4}m^2\end{aligned} \tag{A.1}$$

In the discretized model, enthalpy of sodium chloride solution is evaluated at each computational cell as a function of both local temperature and salinity. In both the discretized and HX models, an average value of membrane permeability coefficient and an average heat transfer coefficient applicable along the lengths of the feed and cold channels are used. Figure A.12 compares the GOR and flux results obtained with the simplified HX-analogy model and 1-D discretized numerical model over the range of system parameters relevant to this study: $v_{\mathrm{f,in}} = 6$–12 cm/s, $L = 1$–6 m, $\delta_\mathrm{m} = 200, 600$ μm, and $s = 60$–260 g/kg. Note that the dotted lines (results of the HX model) closely follow the solid lines (results from 1-D discretized model), and capture the key features of high salinity performance such as the existence of an optimal length beyond which GOR begins to decrease.

Appendix B. Optimal membrane thickness of batch MD at constant feed velocity

Figure B.13 shows the GOR-flux performance curves for a range of δ_m values, along with the upper limit profile, for the case of constant feed velocity of 6 cm/s. The optimal performance curve with velocity control and for continuous recirculation are also reproduced from Fig. 11a. Active velocity control enables a 5–10% higher GOR than the case of constant feed velocity, for large area systems. Note that the optimal membrane thickness for the constant velocity case is higher that the case with velocity control, for the same average flux. If a thicker membrane is more expensive, that could be another reason to opt for velocity control. For a system designed at a specific module length and membrane thickness, reducing the average velocity,

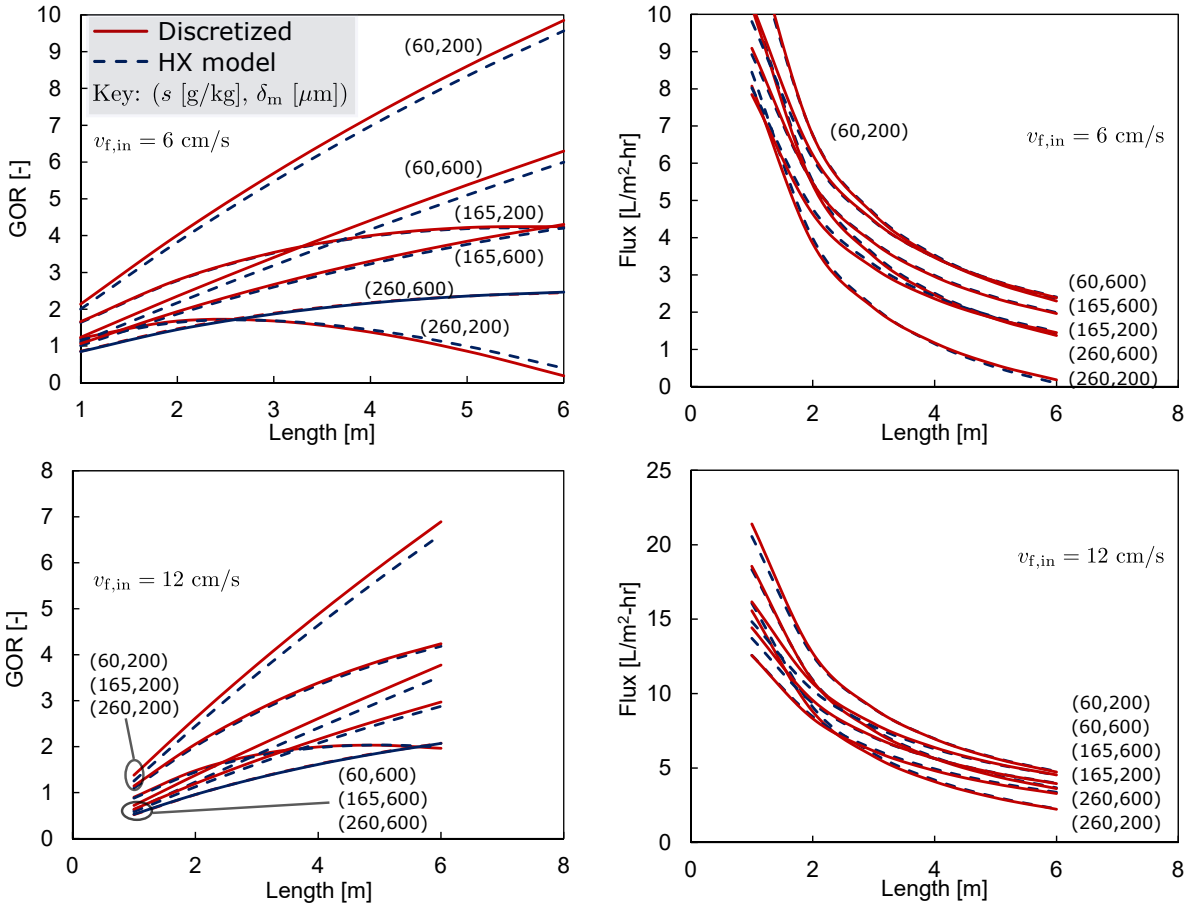

Figure A.12: Comparison of simplified model with full discretized numerical model. The first set of figures compare GOR and flux at feed inlet velocity of 6 cm/s, while varying membrane thickness, module length and salinity, whereas the second set of figures perform the comparison at a higher inlet velocity of 12 cm/s.

allowing for velocity increase towards the end of the cycle time allows to operate at a higher GOR when the treatment load on the system is reduced (so that a lower average flux is sufficient).

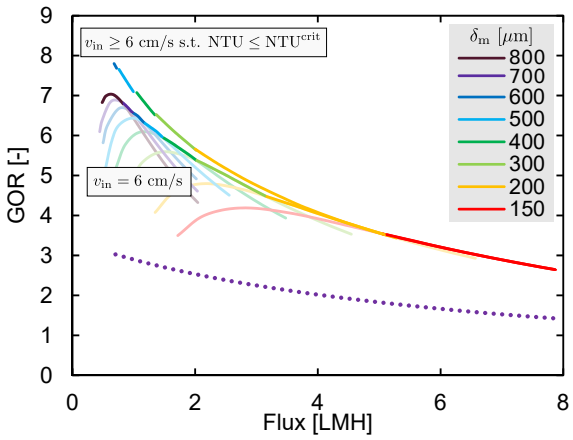

Figure B.13: Optimal membrane thickness for batch RO: constant velocity and variable velocity operation.